# Dijet Production by Double Pomeron Exchange at the Fermilab Tevatron

T. Affolder,[21] H. Akimoto,[43] A. Akopian,[36] M. G. Albrow,[10] P. Amaral,[7] S. R. Amendolia,[32] D. Amidei,[24] K. Anikeev,[22] J. Antos,[1] G. Apollinari,[10] T. Arisawa,[43] T. Asakawa,[41] W. Ashmanskas,[7] M. Atac,[10] F. Azfar,[29] P. Azzi-Bacchetta,[30] N. Bacchetta,[30] M. W. Bailey,[26] S. Bailey,[14] P. de Barbaro,[35] A. Barbaro-Galtieri,[21] V. E. Barnes,[34] B. A. Barnett,[17] M. Barone,[12] G. Bauer,[22] F. Bedeschi,[32] S. Belforte,[40] G. Bellettini,[32] J. Bellinger,[44] D. Benjamin,[9] J. Bensinger,[4] A. Beretvas,[10] J. P. Berge,[10] J. Berryhill,[7] B. Bevensee,[31] A. Bhatti,[36] M. Binkley,[10] D. Bisello,[30] R. E. Blair,[2] C. Blocker,[4] K. Bloom,[24] B. Blumenfeld,[17] S. R. Blusk,[35] A. Bocci,[32] K. Borras,[36] A. Bodek,[35] W. Bokhari,[31] G. Bolla,[34] Y. Bonushkin,[5] D. Bortoletto,[34] J. Boudreau,[33] A. Brandl,[26] S. van den Brink,[17] C. Bromberg,[25] M. Brozovic,[9] N. Bruner,[26] E. Buckley-Geer,[10] J. Budagov,[8] H. S. Budd,[35] K. Burkett,[14] G. Busetto,[30] A. Byon-Wagner,[10] K. L. Byrum,[2] P. Calafiura,[21] M. Campbell,[24] W. Carithers,[21] J. Carlson,[24] D. Carlsmith,[44] J. Cassada,[35] A. Castro,[30] D. Cauz,[40] A. Cerri,[32] A. W. Chan,[1] P. S. Chang,[1] P. T. Chang,[1] J. Chapman,[24] C. Chen,[31] Y. C. Chen,[1] M.-T. Cheng,[1] M. Chertok,[38] G. Chiarelli,[32] I. Chirikov-Zorin,[8] G. Chlachidze,[8] F. Chlebana,[10] L. Christofek,[16] M. L. Chu,[1] C. I. Ciobanu,[27] A. G. Clark,[13] A. Connolly,[21] M. Convery,[36] J. Conway,[37] J. Cooper,[10] M. Cordelli,[12] J. Cranshaw,[39] D. Cronin-Hennessy,[9] R. Cropp,[23] R. Culbertson,[7] D. Dagenhart,[42] F. DeJongh,[10] S. Dell'Agnello,[12] M. Dell'Orso,[32] R. Demina,[10] L. Demortier,[36] M. Deninno,[3] P. F. Derwent,[10] T. Devlin,[37] J. R. Dittmann,[10] S. Donati,[32] J. Done,[38] T. Dorigo,[14] N. Eddy,[16] K. Einsweiler,[21] J. E. Elias,[10] E. Engels, Jr.,[33] W. Erdmann,[10] D. Errede,[16] S. Errede,[16] Q. Fan,[35] R. G. Feild,[45] C. Ferretti,[32] R. D. Field,[11] I. Fiori,[3] B. Flaugher,[10] G. W. Foster,[10] M. Franklin,[14] J. Freeman,[10] J. Friedman,[22] Y. Fukui,[20] S. Galeotti,[32] M. Gallinaro,[36] T. Gao,[31] M. Garcia-Sciveres,[21] A. F. Garfinkel,[34] P. Gatti,[30] C. Gay,[45] S. Geer,[10] D. W. Gerdes,[24] P. Giannetti,[32] V. Glagolev,[8] M. Gold,[26] J. Goldstein,[10] A. Gordon,[14] A. T. Goshaw,[9] Y. Gotra,[33] K. Goulianos,[36] C. Green,[34] L. Groer,[37] C. Grosso-Pilcher,[7] M. Guenther,[34] G. Guillian,[24] J. Guimaraes da Costa,[14] R. S. Guo,[1] R. M. Haas,[11] C. Haber,[21] E. Hafen,[22] S. R. Hahn,[10] C. Hall,[14] T. Handa,[15] R. Handler,[44] W. Hao,[39] F. Happacher,[12] K. Hara,[41] A. D. Hardman,[34] R. M. Harris,[10] F. Hartmann,[18] K. Hatakeyama,[36] J. Hauser,[5] J. Heinrich,[31] A. Heiss,[18] M. Herndon,[17] B. Hinrichsen,[23] K. D. Hoffman,[34] C. Holck,[31] R. Hollebeek,[31] L. Holloway,[16] R. Hughes,[27] J. Huston,[25] J. Huth,[14] H. Ikeda,[41] J. Incandela,[10] G. Introzzi,[32] J. Iwai,[43] Y. Iwata,[15] E. James,[24] H. Jensen,[10] M. Jones,[31] U. Joshi,[10] H. Kambara,[13] T. Kamon,[38] T. Kaneko,[41] K. Karr,[42] H. Kasha,[45] Y. Kato,[28] T. A. Keaffaber,[34] K. Kelley,[22] M. Kelly,[24] R. D. Kennedy,[10] R. Kephart,[10] D. Khazins,[9] T. Kikuchi,[41] B. Kilminster,[35] M. Kirby,[9] M. Kirk,[4] B. J. Kim,[19] D. H. Kim,[19] H. S. Kim,[16] M. J. Kim,[19] S. H. Kim,[41] Y. K. Kim,[21] L. Kirsch,[4] S. Klimenko,[11] P. Koehn,[27] A. Köngeter,[18] K. Kondo,[43] J. Konigsberg,[11] K. Kordas,[23] A. Korn,[22] A. Korytov,[11] E. Kovacs,[2] J. Kroll,[31] M. Kruse,[35] S. E. Kuhlmann,[2] K. Kurino,[15] T. Kuwabara,[41] A. T. Laasanen,[34] N. Lai,[7] S. Lami,[36] S. Lammel,[10] J. I. Lamoureux,[4] M. Lancaster,[21] G. Latino,[32] T. LeCompte,[2] A. M. Lee IV,[9] K. Lee,[39] S. Leone,[32] J. D. Lewis,[10] M. Lindgren,[5] T. M. Liss,[16] J. B. Liu,[35] Y. C. Liu,[1] N. Lockyer,[31] J. Loken,[29] M. Loreti,[30] D. Lucchesi,[30] P. Lukens,[10] S. Lusin,[44] L. Lyons,[29] J. Lys,[21] R. Madrak,[14] K. Maeshima,[10] P. Maksimovic,[14] L. Malferrari,[3] M. Mangano,[32] M. Mariotti,[30] G. Martignon,[30] A. Martin,[45] J. A. J. Matthews,[26] J. Mayer,[23] P. Mazzanti,[3] K. S. McFarland,[35] P. McIntyre,[38] E. McKigney,[31] P. Melese,[36] M. Menguzzato,[30] A. Menzione,[32] C. Mesropian,[36] T. Miao,[10] R. Miller,[25] J. S. Miller,[24] H. Minato,[41] S. Miscetti,[12] M. Mishina,[20] G. Mitselmakher,[11] N. Moggi,[3] C. Moore,[10] E. Moore,[26] R. Moore,[24] Y. Morita,[20] A. Mukherjee,[10] T. Muller,[18] A. Munar,[32] P. Murat,[10] S. Murgia,[25] M. Musy,[40] J. Nachtman,[5] S. Nahn,[45] H. Nakada,[41] T. Nakaya,[7] I. Nakano,[15] C. Nelson,[10] D. Neuberger,[18] C. Newman-Holmes,[10] C.-Y. P. Ngan,[22] P. Nicolaidi,[40] H. Niu,[4] L. Nodulman,[2] A. Nomerotski,[11] S. H. Oh,[9] T. Ohmoto,[15] T. Ohsugi,[15] R. Oishi,[41] T. Okusawa,[28] J. Olsen,[44] W. Orejudos,[21] C. Pagliarone,[32] F. Palmonari,[32] R. Paoletti,[32] V. Papadimitriou,[39] S. P. Pappas,[45] D. Partos,[4] J. Patrick,[10] G. Pauletta,[40] M. Paulini,[21] C. Paus,[22] L. Pescara,[30] T. J. Phillips,[9] G. Piacentino,[32] K. T. Pitts,[16] R. Plunkett,[10] A. Pompos,[34] L. Pondrom,[44] G. Pope,[33] M. Popovic,[23] F. Prokoshin,[8] J. Proudfoot,[2] F. Ptohos,[12] O. Pukhov,[8] G. Punzi,[32] K. Ragan,[23] A. Rakitine,[22] D. Reher,[21] A. Reichold,[29] W. Riegler,[14] A. Ribon,[30] F. Rimondi,[3] L. Ristori,[32] W. J. Robertson,[9] A. Robinson,[23] T. Rodrigo,[6] S. Rolli,[42] L. Rosenson,[22] R. Roser,[10] R. Rossin,[30] W. K. Sakumoto,[35] D. Saltzberg,[5] A. Sansoni,[12] L. Santi,[40] H. Sato,[41] P. Savard,[23] P. Schlabach,[10] E. E. Schmidt,[10] M. P. Schmidt,[45] M. Schmitt,[14] L. Scodellaro,[30] A. Scott,[5] A. Scribano,[32] S. Segler,[10] S. Seidel,[26] Y. Seiya,[41] A. Semenov,[8] F. Semeria,[3] T. Shah,[22] M. D. Shapiro,[21] P. F. Shepard,[33] T. Shibayama,[41] M. Shimojima,[41] M. Shochet,[7] J. Siegrist,[21] G. Signorelli,[32] A. Sill,[39] P. Sinervo,[23] P. Singh,[16] A. J. Slaughter,[45] K. Sliwa,[42] C. Smith,[17] F. D. Snider,[10] A. Solodsky,[36] J. Spalding,[10] T. Speer,[13] P. Sphicas,[22] F. Spinella,[32]

0031-9007/00/85(20)/4215(6)$15.00  

M. Spiropulu,[14] L. Spiegel,[10] J. Steele,[44] A. Stefanini,[32] J. Strologas,[16] F. Strumia,[13] D. Stuart,[10] K. Sumorok,[22] T. Suzuki,[41] T. Takano,[28] R. Takashima,[15] K. Takikawa,[41] P. Tamburello,[9] M. Tanaka,[41] B. Tannenbaum,[5] W. Taylor,[23] M. Tecchio,[24] P. K. Teng,[1] K. Terashi,[41] S. Tether,[22] D. Theriot,[10] R. Thurman-Keup,[2] P. Tipton,[35] S. Tkaczyk,[10] K. Tollefson,[35] A. Tollestrup,[10] H. Toyoda,[28] W. Trischuk,[23] J. F. de Troconiz,[14] J. Tseng,[22] N. Turini,[32] F. Ukegawa,[41] T. Vaiciulis,[35] J. Valls,[37] S. Vejcik III,[10] G. Velev,[10] R. Vidal,[10] R. Vilar,[6] I. Volobouev,[21] D. Vucinic,[22] R. G. Wagner,[2] R. L. Wagner,[10] J. Wahl,[7] N. B. Wallace,[37] A. M. Walsh,[37] C. Wang,[9] C. H. Wang,[1] M. J. Wang,[1] T. Watanabe,[41] D. Waters,[29] T. Watts,[37] R. Webb,[38] H. Wenzel,[18] W. C. Wester III,[10] A. B. Wicklund,[2] E. Wicklund,[10] H. H. Williams,[31] P. Wilson,[10] B. L. Winer,[27] D. Winn,[24] S. Wolbers,[10] D. Wolinski,[24] J. Wolinski,[25] S. Wolinski,[24] S. Worm,[26] X. Wu,[13] J. Wyss,[32] A. Yagil,[10] W. Yao,[21] G. P. Yeh,[10] P. Yeh,[1] J. Yoh,[10] C. Yosef,[25] T. Yoshida,[28] I. Yu,[19] S. Yu,[31] Z. Yu,[45] A. Zanetti,[40] F. Zetti,[21] and S. Zucchelli[3]

(CDF Collaboration)

[1]*Institute of Physics, Academia Sinica, Taipei, Taiwan 11529, Republic of China*
[2]*Argonne National Laboratory, Argonne, Illinois 60439*
[3]*Istituto Nazionale di Fisica Nucleare, University of Bologna, I-40127 Bologna, Italy*
[4]*Brandeis University, Waltham, Massachusetts 02254*
[5]*University of California at Los Angeles, Los Angeles, California 90024*
[6]*Instituto de Fisica de Cantabria, CSIC-University of Cantabria, 39005 Santander, Spain*
[7]*Enrico Fermi Institute, University of Chicago, Chicago, Illinois 60637*
[8]*Joint Institute for Nuclear Research, RU-141980 Dubna, Russia*
[9]*Duke University, Durham, North Carolina 27708*
[10]*Fermi National Accelerator Laboratory, Batavia, Illinois 60510*
[11]*University of Florida, Gainesville, Florida 32611*
[12]*Laboratori Nazionali di Frascati, Istituto Nazionale di Fisica Nucleare, I-00044 Frascati, Italy*
[13]*University of Geneva, CH-1211 Geneva 4, Switzerland*
[14]*Harvard University, Cambridge, Massachusetts 02138*
[15]*Hiroshima University, Higashi-Hiroshima 724, Japan*
[16]*University of Illinois, Urbana, Illinois 61801*
[17]*The Johns Hopkins University, Baltimore, Maryland 21218*
[18]*Institut für Experimentelle Kernphysik, Universität Karlsruhe, 76128 Karlsruhe, Germany*
[19]*Korean Hadron Collider Laboratory, Kyungpook National University, Taegu 702-701, Korea;*
*Seoul National University, Seoul 151-742, Korea;*
*and SungKyunKwan University, Suwon 440-746, Korea*
[20]*High Energy Accelerator Research Organization (KEK), Tsukuba, Ibaraki 305, Japan*
[21]*Ernest Orlando Lawrence Berkeley National Laboratory, Berkeley, California 94720*
[22]*Massachusetts Institute of Technology, Cambridge, Massachusetts 02139*
[23]*Institute of Particle Physics, McGill University, Montreal, Canada H3A 2T8*
*and University of Toronto, Toronto, Canada M5S 1A7*
[24]*University of Michigan, Ann Arbor, Michigan 48109*
[25]*Michigan State University, East Lansing, Michigan 48824*
[26]*University of New Mexico, Albuquerque, New Mexico 87131*
[27]*The Ohio State University, Columbus, Ohio 43210*
[28]*Osaka City University, Osaka 588, Japan*
[29]*University of Oxford OX1 3RH, United Kingdom*
[30]*Universita di Padova, Istituto Nazionale di Fisica Nucleare, Sezione di Padova, I-35131 Padova, Italy*
[31]*University of Pennsylvania, Philadelphia, Pennsylvania 19104*
[32]*Istituto Nazionale di Fisica Nucleare, University and Scuola Normale Superiore of Pisa, I-56100 Pisa, Italy*
[33]*University of Pittsburgh, Pittsburgh, Pennsylvania 15260*
[34]*Purdue University, West Lafayette, Indiana 47907*
[35]*University of Rochester, Rochester, New York 10021*
[36]*Rockefeller University, New York, New York 10021*
[37]*Rutgers University, Piscataway, New Jersey 08855*
[38]*Texas A&M University, College Station, Texas 77843*
[39]*Texas Tech University, Lubbock, Texas 79409*
[40]*Istituto Nazionale di Fisica Nucleare, University of Trieste, Udine, Italy*
[41]*University of Tsukuba, Tsukuba, Ibaraki 305, Japan*
[42]*Tufts University, Medford, Massachusetts 02155*
[43]*Waseda University, Tokyo 169, Japan*
[44]*University of Wisconsin, Madison, Wisconsin 53706*
[45]*Yale University, New Haven, Connecticut 06520*

(Received 8 May 2000)

We report the first observation of dijet events with a double Pomeron exchange topology produced in $\bar{p}p$ collisions at $\sqrt{s} = 1800$ GeV. The events are characterized by a leading antiproton, two jets in the central pseudorapidity region, and a large rapidity gap on the outgoing proton side. We present results on jet kinematics and production rates, compare them with corresponding results from single diffractive and inclusive dijet production, and test factorization.

PACS numbers: 13.87.Ce, 12.38.Qk, 12.40.Nn

In a previous Letter [1], we reported a measurement of the structure function of the antiproton extracted from dijet events produced in single diffractive (SD) $\bar{p}p$ collisions at $\sqrt{s} = 1800$ GeV. Two striking features were noted: (a) the SD structure function rises relative to the nondiffractive (ND) as $x$-Bjorken decreases and (b) it differs from the corresponding structure function of the proton extracted by the H1 Collaboration from measurements of diffractive deep inelastic scattering performed at HERA [2] in both $x$ dependence and normalization. The Fermilab Tevatron to HERA relative normalization was found to be of $\mathcal{O}(0.1)$, confirming our earlier results based on diffractive $W$, dijet, and $b$-quark production rates [3].

The SD event topology for $\bar{p} + p \rightarrow \bar{p}' + \text{jet1} + \text{jet2} + X$ is illustrated in Fig. 1a. It is characterized by a leading antiproton adjacent to a rapidity gap, defined as a region of pseudorapidity [4] devoid of particles. The rapidity gap is presumed to be due to the exchange of a Pomeron, which is viewed here generically as a color singlet with vacuum quantum numbers. The observed difference between the SD structure functions measured at the Fermilab Tevatron and at HERA implies that the Pomeron does not possess a unique hadronlike structure function. This breakdown of factorization is not well understood theoretically, since the processes studied include not only a hard scattering but also nonperturbative exchanges associated with the formation of the rapidity gap. It is generally believed that the formation of rapidity gaps is suppressed in $\bar{p}p$ relative to $\gamma^* p$ collisions due to additional exchanges that spoil the gap [5]. The gap "survival probability" depends on $\sqrt{s}$ and on the presence of additional diffractive gaps, as in the double Pomeron exchange (DPE) event topology shown schematically in Fig. 1b. In this paper, we report the first observation of dijet production by DPE in $\bar{p}p$ collisions at $\sqrt{s} = 1800$ GeV and test factorization by comparing the diffractive structure function measured in SD with that determined from DPE. A previous study of dijet production with a DPE topology in $\bar{p}p$ collisions at $\sqrt{s} = 630$ GeV was performed by a subgroup of the UA1 Collaboration [6], but since the presence of two forward rapidity gaps was required in the trigger it was not conclusively demonstrated that the observed events were due to DPE.

Our DPE signal was extracted from the dijet event sample used in determining the ratio of the $\bar{p}$ diffractive to ND structure functions [1]. The events were collected by triggering on a leading antiproton detected in a forward Roman Pot Spectrometer (RPS). In our SD data analysis we used events from $\bar{p}p$ collisions at $\sqrt{s} = 1800$ GeV containing at least two jets of transverse energy [4] $E_T^{\text{jet}} > 7$ GeV and an antiproton of fractional momentum loss $\xi$ in the range $0.035 < \xi < 0.095$ and 4-momentum transfer squared $|t| < 1$ GeV$^2$. An inclusive dijet sample with the same $E_T^{\text{jet}}$ thresholds, to be referred to from here on as ND, was used as a "reference" against which distributions and rates were gauged. In ratios of SD to ND rates systematic uncertainties from jet energy calibration and detector effects, such as those from energy losses at the interfaces between calorimeters, tend to cancel out. For each event, the values of $x$-Bjorken of the colliding partons of the proton and antiproton were determined using the expressions

$$x_p = \frac{1}{\sqrt{s}} \sum_{i=1}^{N_{\text{jet}}} E_T^i e^{+\eta_i}, \qquad x_{\bar{p}} = \frac{1}{\sqrt{s}} \sum_{i=1}^{N_{\text{jet}}} E_T^i e^{-\eta_i}, \quad (1)$$

where the sum is carried over the two leading (highest transverse energy) jets plus a third jet if $E_T^{\text{jet3}} > 5$ GeV. In leading order QCD, the ratio $R_{\text{ND}}^{\text{SD}}(x_{\bar{p}})$ of the number of SD to ND dijet events (normalized to cross sections) as a function of $x_{\bar{p}}$ is equal to the ratio of the diffractive to ND color weighted structure functions of the antiproton, $F_{jj}(x) = x[g(x) + \frac{4}{9}\sum_i q_i(x)]$, where $g(x)$ and $q(x)$ are gluon and (anti)quark densities, respectively, and $\frac{4}{9}$ is a color factor. Similarly, assuming factorization, the ratio $R_{\text{SD}}^{\text{DPE}}(x_p)$ of the DPE to SD rates should be equal to the ratio of the diffractive to ND structure functions of the proton. A deviation of the double ratio $D \equiv R_{\text{ND}}^{\text{SD}}(x_{\bar{p}})/R_{\text{SD}}^{\text{DPE}}(x_p)$ from unity would therefore indicate a breakdown of factorization.

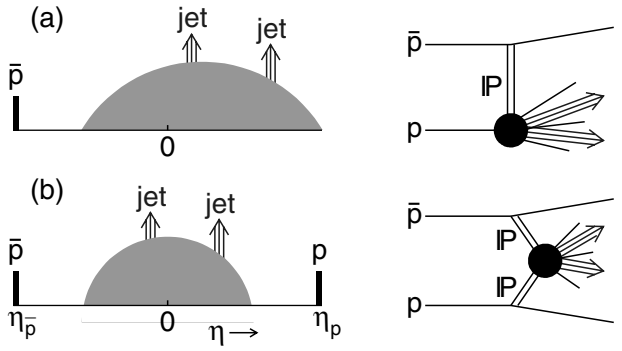


FIG. 1. Illustration of event topologies in pseudorapidity, $\eta$, and associated Pomeron exchange diagrams for dijet production in (a) single diffraction and (b) double Pomeron exchange. The shaded areas on the left side represent particles not associated with the jets (underlying event).

The components of the CDF detector [7] relevant to this analysis are, in addition to the RPS, the central/vertex tracking chambers (CTC, VTX), the calorimeters (CAL), and the beam-beam counters (BBC), covering the regions $|\eta| < 1.8$, $|\eta| < 4.2$, and $3.2 < |\eta| < 5.9$, respectively. The tracking chambers allow us to determine the event vertex and select events due to a single interaction; the calorimeters are used to measure the energies and $\eta$-$\phi$ positions of particles and jets; and the BBC's, which are sensitive only to charged particles, are used in combination with the forward calorimeters (FCAL, $2.4 < |\eta| < 4.2$) to detect forward rapidity gaps.

Our SD (ND) data set [1] consists of 30 439 (32 629) events containing at least two jets with corrected $E_T^{\rm jet} > 7$ GeV. The $E_T$ of a jet is defined as the sum of calorimeter towers with $E_T$ above 100 MeV within an $\eta$-$\phi$ cone of radius 0.7. The correction to the jet $E_T$ includes a subtraction of 0.54 (1.16) GeV to account for the underlying event energy in SD (ND) events. The SD events are required to have a single vertex within $|z_{\rm vtx}| < 60$ cm. Despite the vertex requirement, a study of BBC hit and FCAL tower multiplicity distributions showed that $\approx$7% of the events in our SD data set were due to multiple interactions. In the present analysis, these *overlap* events are rejected by requiring the number of BBC hits on the $\bar{p}$ side to be $N_{{\rm BBC}\bar{p}} \leq 6$. The remaining sample contains 27 405 events. The residual overlap background in this sample is estimated to be $(0.5 \pm 0.2)$%.

Using the SD data set, we searched for a DPE signal characterized by events with a rapidity gap on the outgoing proton side (positive $\eta$). Figure 2a shows the correlation between BBC hits, $N_{{\rm BBC}p}$, and adjacent FCAL towers with (corrected) energy $E > 1.5$ GeV [3], $N_{{\rm FCAL}p}$. The clear excess in the (0,0) bin above a smooth extrapolation from nearby bins is attributed to events with a rapidity gap due to DPE. The average underlying event energy of the data in this bin was found to be 0.37 GeV. The plot in Fig. 2a was actually obtained by a second pass through the SD event sample, in which an underlying event energy of 0.37 GeV was used in the jet energy correction. The SD component of the (0,0) bin, which contains 132 events, is evaluated from the distribution of events along the diagonal bins with $N_{{\rm BBC}p} = N_{{\rm FCAL}p}$, shown in Fig. 2b. An extrapolation to bin (0,0) of a linear fit to the data of bins (2,2) to (10,10) yields $14.3 \pm 11.0$(syst-fit) SD background events.

Figure 2c shows the $\xi_{\bar{p}}$ distributions, corrected for RPS acceptance, of the DPE [(0,0) bin] (points) and SD (histogram) event samples. Qualitatively, the observed rise of the DPE relative to the SD distribution with increasing $\xi_{\bar{p}}$ may be explained by the lower c.m. subsystem energy of the DPE events and the steep $x$ dependence of the diffractive $\bar{p}$ structure function [1].

The $\xi_p$ ($\xi_{\bar{p}}$) of the (anti)proton in DPE can be determined from Eq. (1) by replacing $x$ by $\xi$ and summing over all particles in the event, both charged and neutral. Detector inefficiencies and particles with $E_T$ below tower threshold are accounted for by multiplying the result by 1.7. This

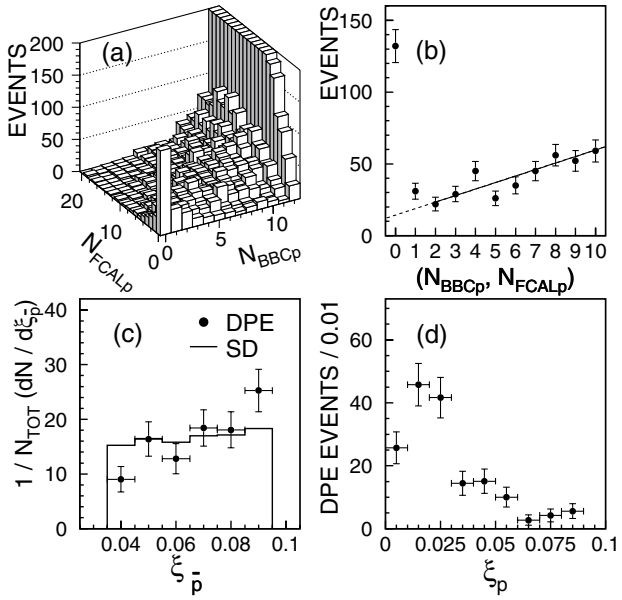


FIG. 2. (a) Beam-beam counter hit multiplicity on the proton side, $N_{{\rm BBC}p}$, versus forward calorimeter tower multiplicity, $N_{{\rm FCAL}p}$: the peak in the (0,0) bin contains the DPE signal; (b) multiplicity distribution along the diagonal bins in (a) with $N_{{\rm BBC}p} = N_{{\rm FCAL}p}$; (c) $\xi_{\bar{p}}$ measured by the RPS for SD events (histogram) and for the "DPE" events of the (0,0) bin in (a); (d) $\xi_p$ of the DPE events. In (c) and (d) the data are corrected for RPS acceptance on an event-by-event basis.

calibration factor was evaluated by comparing the value of $\xi_{\bar{p}}$ obtained using the above procedure with that determined by the RPS (with an accuracy of $\delta\xi = 0.001$) using SD events with $N_{{\rm BBC}\bar{p}} = N_{{\rm FCAL}\bar{p}} = 0$. The $\xi_p$ distribution for the DPE events is shown in Fig. 2d. The events are concentrated in the region $0.01 < \xi_p < 0.03$.

In Fig. 3 we compare distributions of mean dijet transverse energy, $E_T^* = (E_T^1 + E_T^2)/2$, mean pseudorapidity, $\eta^* = (\eta_1 + \eta_2)/2$, azimuthal angle difference, $\phi = |\phi_1 - \phi_2|$, and dijet mass fraction for DPE (points), SD (solid histograms), and ND (dashed) events. The dijet mass fraction, $R_{jj/X}$, is defined as the mass of the dijet system evaluated using only the energy within the cones of the two leading jets, $M_{jj}^{\rm cone}$, divided by the mass of the central system, $M_X = (s\xi_p\xi_{\bar{p}}^{\rm RPS})^{1/2}$. For the SD and ND cases we use $M_X = (s\xi_{\bar{p}}^{\rm RPS})^{1/2}$ and $s^{1/2}$, respectively. For DPE events in which the dijet mass accounts for the total mass of the central system (no underlying event energy), the dijet mass fraction, which is based on jet energies with no out-of-cone energy corrections, is expected to be in the region $0.7 < R_{jj/X} < 0.9$, as shown by the shaded histogram in Fig. 3d. We observe no events in the region of $R_{jj/X} > 0.7$. However, considering all systematic uncertainties that can cause shifts in the measured $R_{jj/X}$ values yield one such event, on the basis of which we set a 95% C.L. upper bound of 5.1 events.

The data of the (0,0) bin of Fig. 2a must be corrected for the efficiency of the BBC$\bar{p}$ multiplicity cut, $f_{{\rm BBC}\bar{p}}$, the single vertex cut efficiency, $f_{\rm vtx}$, the BBC$p$/FCAL$p$

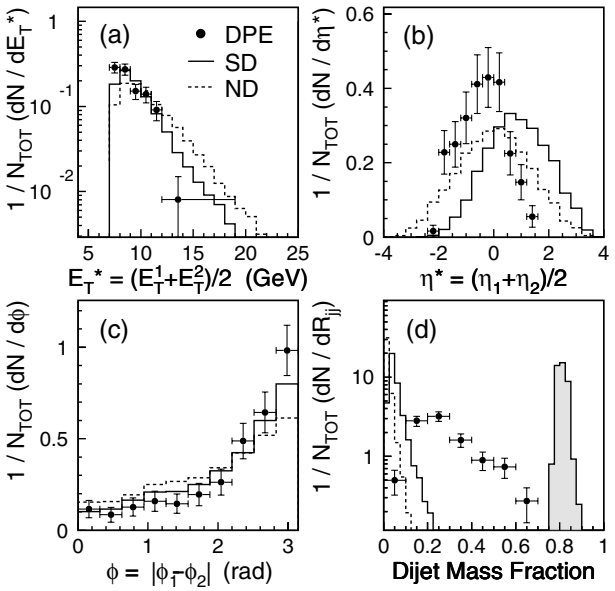


FIG. 3. Distributions for DPE events [(0,0) bin in Fig. 2] (points) compared with corresponding single diffractive (nondiffractive) distributions shown as solid (dashed) histograms: (a) mean jet $E_T$, (b) mean $\eta$ of the dijet system, (c) azimuthal angle difference between the two leading jets, and (d) ratio of dijet mass obtained from the energies within jet cones of $\eta$-$\phi$ radius 0.7 to total central system mass. The shaded histogram shows the expected mass fraction for events in which the dijet mass accounts for the total mass of the central system.

livetime acceptance, $f_{\rm live}$, and the rapidity gap acceptance, $f_{\rm RG}$, defined as the ratio of the DPE events with a rapidity gap on the $p$ side to the total number of DPE events within a given $\xi_p$ range. Analyzing the data without the $N_{\rm BBC\bar{p}} \leq 6$ cut yields 8.5 more DPE events, from which we obtain $f_{\rm BBC}p = (93 \pm 4)\%$. The single vertex requirement, which is imposed to reject events due to multiple interactions, also rejects single interaction events with extra (fake) vertices due to track reconstruction ambiguities. Removing this requirement we obtain 5.1 more DPE events, yielding $f_{\rm vtx} = (96 \pm 3)\%$. By measuring the probability of finding $N_{\rm BBC}p = N_{\rm FCAL}p = 0$ in events with no reconstructed vertex collected by triggering only on beam-beam crossings, we determined the BBC$p$/FCAL$p$ livetime fraction to be $f_{\rm live} = (97 \pm 3)\%$. Finally, from studies of the correlation between the $\xi_p$ and the BBC$p$ and FCAL$p$ multiplicities, the rapidity gap acceptance for events with $0.01 < \xi_p < 0.03$ was found to be $f_{\rm RG} = (84 \pm 11)\%$.

To test factorization, we compare the ratio $R_{\rm SD}^{\rm DPE}(x_p)$ with our previously measured [1] ratio $R_{\rm ND}^{\rm SD}(x_{\bar{p}})$ at $x_p = x_{\bar{p}} \equiv x$ as a function of $x$. For this comparison, we restrict the data to the regions $7 < E_T^{\rm jet1,2} < 10$ GeV, $|t_{\bar{p}}| < 1$ GeV$^2$, $0.035 < \xi_{\bar{p}} < 0.095$, and for DPE $0.01 < \xi_p < 0.03$. In the chosen $\xi_p$ range, the SD background in the DPE candidate event sample is negligibly small. The two ratios, normalized per unit $\xi$, are shown in Fig. 4. The errors are statistical only. The SD/ND ratio has a normalization systematic uncertainty of $\pm 20\%$. The vertical dashed lines mark the DPE kinematic boundary (left) and the value of $x = \xi_p^{\rm min}$ (right). The weighted average of the DPE/SD points in the region within the vertical dashed lines is $\tilde{R}_{\rm SD}^{\rm DPE} = 0.80 \pm 0.26$. Factorization demands that $\tilde{R}_{\rm SD}^{\rm DPE}$ be the same as $\tilde{R}_{\rm ND}^{\rm SD}$ at fixed $x$ and $\xi$. Since the $\xi_p$ and $\xi_{\bar{p}}$ regions, which are respectively relevant for the DPE/SD and SD/ND ratios, do not overlap, we examine in the inset in Fig. 4 the $\xi$ dependence of the ratios $\tilde{R}(x)$ (per unit $\xi$), where the tilde over the $R$ indicates the weighted average of the points in the region of $x$ within the vertical dashed lines in the main figure. The ratio $\tilde{R}_{\rm ND}^{\rm SD}$, shown in six $\xi$ bins in the region $0.035 < \xi < 0.095$, is flat in $\xi$. A straight line fit to the six $\tilde{R}_{\rm ND}^{\rm SD}$ ratios extrapolated to $\xi = 0.02$ yields $\tilde{R}_{\rm ND}^{\rm SD} = 0.15 \pm 0.02$. The ratio of $\tilde{R}_{\rm ND}^{\rm SD}$ to $\tilde{R}_{\rm SD}^{\rm DPE}$ is $D \equiv \tilde{R}_{\rm ND}^{\rm SD}/\tilde{R}_{\rm SD}^{\rm DPE} = 0.19 \pm 0.07$. The deviation of $D$ from unity represents a breakdown of factorization.

Focusing on the proton side in Fig. 1, DPE/SD at $\sqrt{s}$ may be viewed as SD/ND at the diffractive mass energy of $\sqrt{\xi_{\bar{p}} s}$, which is reduced relative to $\sqrt{s}$ due to the presence of the gap on the antiproton side. This situation is analogous to the suppression of hard diffraction rates observed at the Fermilab Tevatron [1,3] relative to expectations based on the lower energy diffractive deep inelastic scattering measurements at HERA. Thus, it appears that $D$ decreases as the energy, or equivalently the $\eta$ range available for the formation of a rapidity gap increases. Such behavior is expected by the (re)normalized gap probability model [8], as well as by models based on rapidity gap survival probability [5].

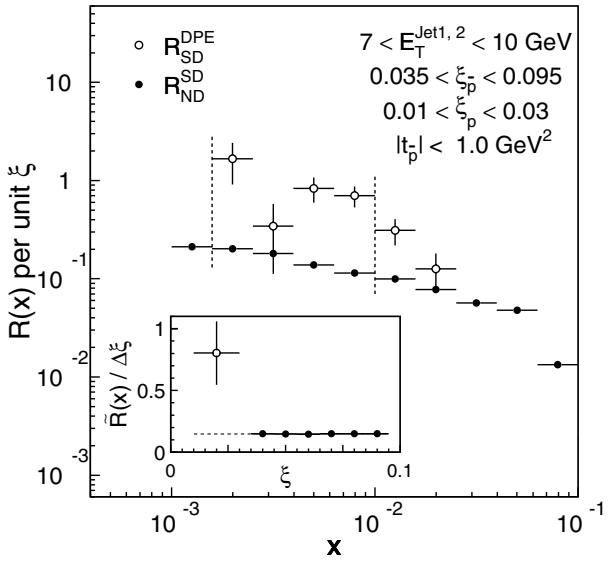


FIG. 4. Ratios of DPE to SD (SD to ND) dijet event rates per unit $\xi_p$ ($\xi_{\bar{p}}$), shown as open (filled) circles, as a function $x$-Bjorken of partons in the $p$ ($\bar{p}$). The errors are statistical only. The SD/ND ratio has a normalization systematic uncertainty of $\pm 20\%$. The inset shows $\tilde{R}(x)$ per unit $\xi$ versus $\xi$, where the tilde over the $R$ indicates the weighted average of the $R(x)$ points in the region of $x$ within the vertical dashed lines, which mark the DPE kinematic boundary (left) and the value of $x = \xi_p^{\rm min}$ (right).

The absolute DPE dijet cross section is obtained by multiplying the DPE/SD ratio by the SD dijet cross section, which is normalized by scaling to the measured [9] inclusive (soft) cross section of $0.78 \pm 0.16$ mb. For $0.035 < \xi_{\bar{p}} < 0.095$, $0.01 < \xi_p < 0.03$, $|t_{\bar{p}}| < 1$ GeV$^2$, and jets of $E_T > 7$ [$E_T > 10$] GeV confined within $-4.2 < \eta < 2.4$, we obtain $\sigma^{\mathrm{DPE}} = 43.6 \pm 4.4(\mathrm{stat}) \pm 21.6(\mathrm{syst})$ [$3.4 \pm 1.0(\mathrm{stat}) \pm 2.0(\mathrm{syst})$] nb, where the systematic errors are dominated by the uncertainties in normalization (20%) and jet energy calibration (40%). In terms of an absolute cross section, the 95% C.L. upper bound we obtained for events in which the jet energies could account for the total energy of the central system corresponds to 3.7 nb. Theoretical estimates of this cross section range from $\sim 10^3$ larger [10] to a few times smaller [11] values than the measured upper bound.

In summary, in a sample of events containing two jets of $E_T^{\mathrm{jet}} > 7$ GeV and a leading antiproton of fractional momentum loss $0.035 < \xi_{\bar{p}} < 0.095$ produced in $\bar{p}p$ collisions at $\sqrt{s} = 1800$ GeV, we have observed a class of events with a double Pomeron exchange topology, characterized by a rapidity gap on the outgoing proton side corresponding to $0.01 < \xi_p < 0.03$. Distributions of jet transverse energy, pseudorapidity, and two-jet azimuthal angle difference were compared with corresponding single diffractive and nondiffractive distributions. Using measured jet kinematical variables, the ratio of double Pomeron exchange to single diffractive rates was determined as a function of $x_p$-Bjorken and compared with the ratio of single diffractive to nondiffractive rates versus $x_{\bar{p}}$ to test factorization. We find a breakdown of factorization, which is quantified by the deviation from unity of the ratio of the SD/ND to DPE/SD rates, $D = 0.19 \pm 0.07$. Based on the observation of one DPE event in which the jet energies could account for the entire energy of the central system, we set a 95% C.L. upper bound of 3.7 nb for such events for our kinematic range of $0.035 < \xi_{\bar{p}} < 0.095$ and jets of $E_T > 7$ GeV confined within $-4.2 < \eta < 2.4$.

We thank the Fermilab staff and the technical staffs of the participating institutions for their vital contributions. This work was supported by the U.S. Department of Energy and National Science Foundation; the Italian Istituto Nazionale di Fisica Nucleare; the Ministry of Education, Science and Culture of Japan; the Natural Sciences and Engineering Research Council of Canada; the National Science Council of the Republic of China; the A. P. Sloan Foundation; the Max Kade Foundation; and the Ministry of Education, Science and Research of the Federal State Nordrhein-Westfalen of Germany.

[1] T. Affolder *et al.,* Phys. Rev. Lett. **84**, 5043 (2000).
[2] T. Ahmed *et al.,* Phys. Lett. B **348**, 681 (1995); C. Adloff *et al.,* Z. Phys. C **76**, 613 (1997); Phys. Lett. B **428**, 206 (1998); Eur. Phys. J. C **6**, 421 (1999).
[3] F. Abe *et al.,* Phys. Rev. Lett. **78**, 2698 (1997); **79**, 2636 (1997); T. Affolder *et al.,* Phys. Rev. Lett. **84**, 232 (2000).
[4] The pseudorapidity, $\eta$, is defined as $\eta = -\ln(\tan\frac{\theta}{2})$, where $\theta$ is the polar angle between a particle or jet and the proton beam direction. The transverse energy of a jet, $E_T^{\mathrm{jet}}$, is given by $E_T^{\mathrm{jet}} = E^{\mathrm{jet}} \sin\theta$.
[5] See, for example, E. Gotsman, E. M. Levin, and U. Maor, Phys. Lett. B **438**, 229 (1998); Phys. Rev. D **60**, 094011 (1999).
[6] D. Joyce *et al.,* Phys. Rev. D **48**, 1943 (1993).
[7] F. Abe *et al.,* Nucl. Instrum. Methods Phys. Res., Sect. A **271**, 387 (1988).
[8] K. Goulianos, Phys. Lett. B **358**, 379 (1995); **363**, 268 (1995); in *Proceedings of LAFEX International School of High Energy Physics, Rio de Janeiro, Brazil, 1998,* CD-ROM LISHEP98, edited by Andrew Brandt, Hélio da Motta, and Alberto Santoro (Industria Brasileira, Rio de Janeiro, 1998); hep-ph/9806384.
[9] F. Abe *et al.,* Phys. Rev. D **50**, 5550 (1994).
[10] A. Berera, Phys. Rev. D **62**, 014015 (2000).
[11] V. A. Khose, A. D. Martin, and M. G. Ryskin, hep-ph/0006005.